

Network Modeling of Aperture-Coupled Vertically Mounted Slotline Coupling Structure

Jeong-Phill Kim, *Member, IEEE*, Il-Bong Jeong, and Cheol-Hoo Kim

Abstract—A general analysis of a microstrip-to-vertically mounted slotline (VMS) coupling structure is presented with a view to developing an equivalent circuit, and the efficient evaluation of the related circuit element values is described. To check the validity of the proposed analysis and design theory, a C-band linearly tapered slot antenna fed by an aperture-coupled microstripline-to-VMS coupling structure is optimally designed, and its computed characteristics, derived from the network analysis, are compared with measurement and simulation results. Reasonable agreement was observed, fully validating the efficiency and accuracy of the proposed network model.

Index Terms—Coupling structure, equivalent circuit, microstripline, slotline, vertically mounted slotline.

I. INTRODUCTION

THERE has been increasing demand for more efficient feeding structures in microwave and millimeter-wave circuit and antenna configurations to enable better performance and easy fabrication. In the development of phased array antennas with tapered slot antenna (TSA) radiating elements [1], coaxial or microstrip line feeds have been widely used. However, they have drawbacks with respect to fabrication and maintenance. To circumvent these problems, an orthogonal feed technique incorporating a microstrip-to-VMS coupling structure has been suggested [2]. However, most design work has been undertaken using experiments or time-consuming numerical analysis.

This paper presents a general analysis of an aperture-coupled microstrip-to-VMS coupling structure with a view to developing an equivalent circuit. To check the validity of the proposed analysis and design theory, a C-band TSA fed by this coupling structure is designed, and its computed characteristics, as derived from the equivalent network model, are compared with measurement and numerical simulation results.

II. ANALYSIS AND NETWORK MODEL

An aperture-coupled microstripline-to-VMS coupling structure comprises a microstripline, a narrow rectangular aperture on the ground plane, and a VMS on the ground plane, as shown in Fig. 1. W_m and S_c denote the width of the microstripline and the VMS, respectively. L_a and W_a are the length and width of the aperture. The substrate thickness and dielectric constant of

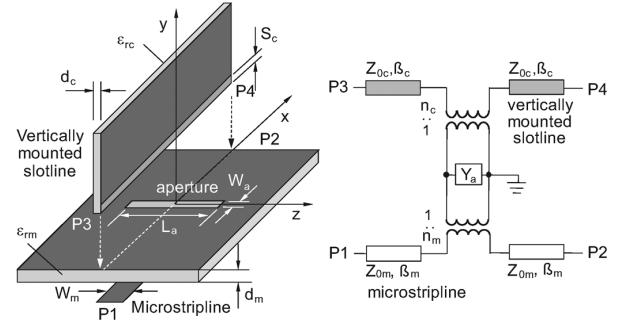


Fig. 1. Structure and equivalent circuit of aperture-coupled microstripline to VMS coupler.

the microstripline are denoted by d_m and ϵ_{rm} , and those of the VMS by d_c and ϵ_{rc} , respectively.

Whereas an equivalent-circuit model showing the coupling effect between the microstripline and the aperture has been well studied [4], to the authors' knowledge there has been no modeling of the coupling between the aperture and the VMS. Even though the VMS configuration is not common, it is simply a transmission line. Therefore, the related coupling can be modeled similarly to that of the microstripline to the aperture. The resulting equivalent circuit can be represented as shown in Fig. 1, where Z_{0m} and β_m denote the characteristic impedance and phase constant of the microstripline, and Z_{0c} and β_c to those of the VMS. Considering the electromagnetic relation between a VMS and a conventional slotline, $Z_{0c} = Z_{0s}/2$ and $\beta_c = \beta_s$, where Z_{0s} and β_s are the characteristic impedance and phase constant of a conventional slotline of width $S = 2S_c$. The aperture admittance is denoted by Y_a , which can be efficiently calculated using a complex power representation in the spectral domain [3]. To complete the coupling analysis, only the turns ratio n_c remains to be evaluated.

Assume that a voltage V_a is applied across the coupling aperture. Then the aperture electric field can be expressed as $\vec{E}_a = -\hat{x}V_a e_{ax}$, where e_{ax} is the x -component of a normalized electric field. Applying the reciprocity theorem [4]–[6] yields the following expression for n_c

$$n_c = \frac{V_c}{P_c} \int_{S_a} e_{ax} h_{cz} \cos(\beta_c x) dS \quad (1)$$

where S_a is the coupling aperture area. V_c , P_c , and h_{cz} denote the voltage, power flow, and z -component of the magnetic field of the VMS, respectively, for an assumed traveling voltage V_c . In evaluating n_c , V_c can be chosen freely. Choosing $V_c = 0.5$ V results in $V_c/P_c = 2Z_{0c} = Z_{0s}$.

Manuscript received June 29, 2009; revised September 07, 2009. First published December 08, 2009; current version published January 08, 2010.

The authors are with the School of Electrical and Electronic Engineering, Chung-Ang University, Seoul 156-756, Korea (e-mail: phill@cau.ac.kr).

Digital Object Identifier 10.1109/LMWC.2009.2035950

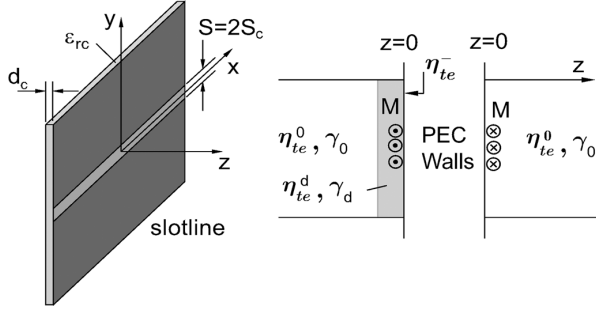


Fig. 2. Structure and transmission line representation of slotline.

For the case of a narrow rectangular aperture that is smaller than the resonant length, e_{ax} can be reasonably approximated by $e_{ax} = f(x)g(z)$, with

$$f(x) = \frac{1}{\pi \sqrt{(W_a/2)^2 - x^2}}, \quad g(z) = \cos\left(\frac{\pi z}{L_a}\right). \quad (2)$$

Now (1) can be recast as $n_c = Z_{0s} I_f I_g$, with

$$I_f = \int_{-W_a/2}^{W_a/2} f(x) \cos(\beta_c x) dx = J_0\left(\frac{W_a \beta_c}{2}\right) \quad (3)$$

$$I_g = \int_{-L_a/2}^{L_a/2} g(z) h_{cz}(y=0, z) dz \quad (4)$$

where $J_0(\cdot)$ is a 0th-order Bessel function of the first kind, and h_{cz} is the z -component of the magnetic field in the VMS for the assumed traveling voltage V_c . To calculate the integral I_g , the value of h_{cz} ($y=0, z$) should be known beforehand.

As mentioned above, the related electromagnetic fields for a VMS line and a conventional slotline (Fig. 2) are the same. Because the related structure is planar on the xy -plane, h_{cz} ($y=0, z$) can be found efficiently in the spectral domain, and I_g can, therefore, be expressed as

$$I_g = \frac{1}{2\pi} \int_{-\infty}^{+\infty} \int_{-L_a/2}^{L_a/2} g(z) \tilde{h}_{cz}(k_y, z) dz dk_y \quad (5)$$

where $\tilde{h}_{cz}(k_y, z)$ is the spectral-domain representation of $h_{cz}(y, z)$. From Maxwell's equations, $\tilde{h}_z(k_y, z)$ can be expressed with the help of the spectral-domain immittance approach (u, v -coordinates) [7] as

$$\begin{aligned} \tilde{h}_z(k_y, z) &= \frac{-k_\rho}{\omega\mu} \tilde{E}_u(k_y, z=0) T(k_y, z) \\ T(k_y, z) &= \begin{cases} e^{-\gamma_0 z}, & z \in z_1 \\ T_d(k_y, z), & z \in z_2 \\ e^{-\gamma_0 |z+d_c|} T_d(k_y, z=-d_c), & z \in z_3 \end{cases} \end{aligned} \quad (6)$$

where $k_\rho = \sqrt{\beta_s^2 + k_y^2}$, $T_d(k_y, z) = \cosh(\gamma_d |z|) - (\eta_{te}^d / \eta_{te}^0) \sinh(\gamma_d |z|)$ and $z_1 = [0, L_a/2]$, $z_2 = [-d_c, 0]$, $z_3 = [-L_a/2, -d_c]$. The subscripts “0” and “d” refer to air and dielectric substrates, respectively. The other related impedance and propagation parameters for the TE_z mode

(Fig. 2) are $\eta_{te}^i = j\omega\mu/\gamma_i$, $\gamma_i^2 = \beta_s^2 + k_y^2 - k_i^2$ ($i=0, d$), and $\eta_{te}^- = \eta_{te}^d (\eta_{te}^0 + \eta_{te}^d \tanh \gamma_d d_c) / (\eta_{te}^0 + \eta_{te}^d \tanh \gamma_d d_c)$.

Because $V_c = 0.5$ V was assumed in the above formulation, the electric field of the slotline at the $z=0$ plane, \tilde{E}_s , can be approximated by $\tilde{E}_s = -\hat{y}/(\pi\sqrt{S_c^2 - y^2})$. Therefore, $\tilde{E}_u(k_y, z=0)$ is given by

$$\tilde{E}_u(k_y, z=0) = \frac{-\beta_s}{k_\rho} \tilde{E}_{sx}(k_y) = \frac{\beta_s}{k_\rho} J_0(S_c k_y). \quad (8)$$

Finally, the resulting $\tilde{h}_z(k_y, z)$ is expressed as

$$\tilde{h}_z(k_y, z) = \frac{\beta_s}{\omega\mu} J_0(S_c k_y) T(k_y, z) \quad (9)$$

and the expression of I_g becomes

$$I_g = \frac{1}{2\pi} \int_{-\infty}^{+\infty} \frac{\beta_s}{\omega\mu} J_0(S_c k_y) G(k_y) dk_y \quad (10)$$

$$G(k_y) = \int_{-L_a/2}^{L_a/2} T(k_y, z) g(z) dz. \quad (11)$$

Because a closed-form expression for $G(k_y)$ exists [8], I_g becomes a 1-D integral with k_y as the only variable. Furthermore, the integrand of I_g has no singularities along the real k_y -axis and decays rapidly, thereby enabling the integral to be calculated numerically without difficulty.

III. RESULTS AND DISCUSSION

To validate the present theory, it is worthwhile to examine the characteristics of an aperture-coupled microstripline-to-VMS. The assumed structure parameter values are $d_m = d_c = 31$ mils, $\epsilon_{rc} = \epsilon_{rm} = 2.2$, $W_a = 0.5$ mm, $S_c = 0.3$ mm, and $W_m = 2.4$ mm. For this case, the propagation characteristics become $Z_{0c} \simeq 59.40 \Omega$ and $\epsilon_{rce} = (\beta_c/\beta_0)^2 \simeq 1.15$ over the frequency range of 3~7 GHz.

Now, n_m , n_c , and the normalized reactance $x_a (= X_a/50)$ are calculated as a function of frequency for $L_a = 10$ mm, giving the results depicted in Fig. 3. For comparison, calculated turns ratios based on the piecewise sinusoidal (PWS) distribution for $g(z)$ given in (2) are also displayed. Because the aperture can be regarded as a slotline resonator, as mentioned above, the reactance increases with increasing frequency. In contrast, the turns ratios n_m and n_c remain nearly constant with increasing frequency.

Using these circuit values, the characteristics of the coupler were calculated and are depicted in Fig. 3. As shown in this figure, the results based on the cosine distribution show better agreement with the numerical simulation than do the PWS-based results. Considering the electric field distribution for the aperture, the electric fields coupled from the aperture to ports 3 and 4 are formed out of phase with each other. Therefore, $S_{41} \simeq -S_{31}$ holds. As shown in Fig. 3, the computed results from the present theory agree well with those of numerical simulation [9]. Increased aperture reactance as the frequency increases results in decreased transmission (S_{21} and S_{43}), increased coupling (S_{31}), and increased return loss (S_{11} and S_{33}).

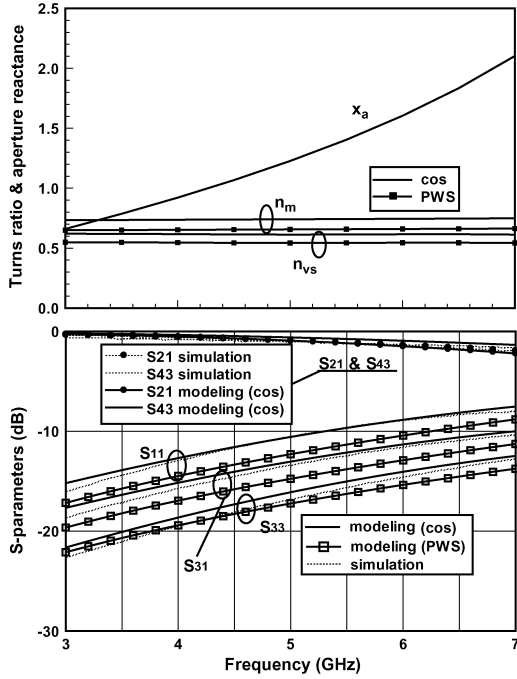


Fig. 3. Circuit element values and characteristics of the coupler as a function of frequency.

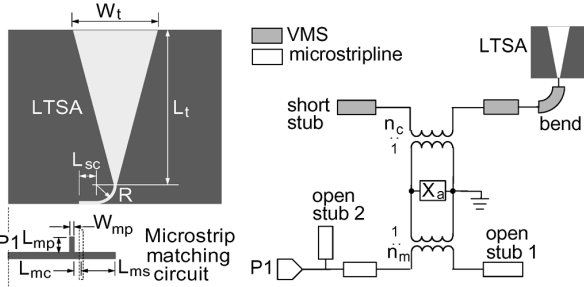


Fig. 4. Configuration and equivalent circuit of LTSA fed by aperture-coupled microstrip-VMS coupling structure.

To validate further the present theory, experimental measurements were made. Because it is not easy to terminate ports 3 and 4 of a VMS, a C-band linearly tapered slot antenna (LTSA) was formed at one end of the VMS, with the other end being shorted, as shown in Fig. 4. Design guidelines for LTSAs are well described in the published literature [1], [10]. An LTSA with $L_t = 46.85$ mm and $W_t = 20.00$ mm on a dielectric substrate ($d_c = 31$ mils and $\epsilon_{rc} = 2.2$) was chosen for this experiment. The slotline connected to the input of the LTSA was bent with a radius of curvature $R = 5$ mm, and was shorted after being extended. The width and length of the coupling aperture were $W_a = 0.50$ mm and $L_a = 10.00$ mm. With these structural parameter values, the characteristics of the LTSA, the slotline bend, and the shorted end were calculated by numerical analysis. Incorporating the numerical simulation data into the equivalent network, as shown in Fig. 4, the remaining design parameters were determined optimally for impedance matching at $f = 5$ GHz [11]. The results were $L_{sc} = 4.35$ mm, $L_{ms} = 9.85$ mm, $L_{mp} = 5.80$ mm, $W_{mp} = 2.00$ mm, $L_{mc} = 1.00$ mm, and $R = 5.00$ mm. The return loss of the fabricated antenna was measured, and it is shown in Fig. 5, together with the computed results from the present network model and the

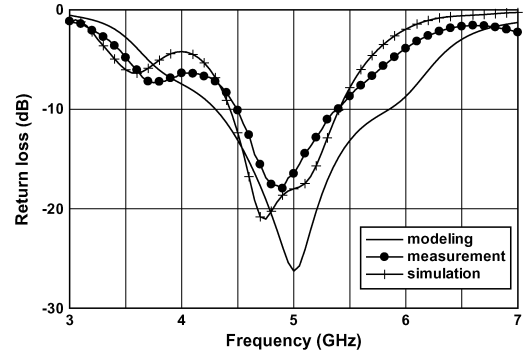


Fig. 5. Characteristics of LTSA fed by aperture-coupled microstrip-VMS coupling structure.

numerical analysis data. Reasonable agreement is observed. Related electrical length of aperture and matching stubs are below the resonant length over the frequency of interest, and the calculated insertion loss was less than 1.81 dB from 4.5 to 5.5 GHz. The results for this example show fully the validity of the proposed theory, and the present network model can, therefore, be widely used in the computer-aided design of related circuits and antennas.

IV. CONCLUSION

A general analysis of a microstrip-to-VMS coupling structure was presented and an equivalent-network model was developed. The equivalent network comprises corresponding lines, two ideal transformers, and a reactive circuit element. The efficient evaluation of the turns ratio for an ideal transformer, which reflects the coupling effect between the aperture and the VMS, was described. To validate the proposed analysis and design theory, a C-band LTSA fed by an aperture-coupled microstrip-to-VMS coupler was optimally designed, and its characteristics, computed from the network analysis, were compared with measurement and simulation results. Reasonable agreement was observed, which fully validates the efficiency and accuracy of the proposed network model.

REFERENCES

- [1] J. Gibson, "The Vivaldi aerial," in *Proc. 9th EUMC, Brighton, U.K.*, 1979, pp. 101–105.
- [2] R. Q. Lee and R. N. Simons, "Orthogonal feeding techniques for tapered slot antennas," in *Proc. IEEE Antennas and Propagation Society Int. Symp.*, 1998, pp. 1172–1175.
- [3] J. P. Kim and W. S. Park, "Network modeling of an inclined and off-center microstrip-fed slot antenna," *IEEE Trans. Antennas Propagat.*, vol. 46, no. 8, pp. 1182–1188, Dec. 1998.
- [4] J. P. Kim and W. S. Park, "An improved network modeling of slot-coupled microstrip lines," *IEEE Trans. Microw. Theory Tech.*, vol. 46, no. 10, pp. 1484–1491, Oct. 1998.
- [5] R. F. Harrington, *Time Harmonic Electromagnetic Fields*. New York: McGraw-Hill, 1961.
- [6] D. M. Pozar, "Reciprocity method of analysis for printed slot and slot-coupled microstrip antennas," *IEEE Trans. Antennas Propagat.*, vol. AP-34, no. 12, pp. 1439–1446, Dec. 1986.
- [7] T. Itoh, "Spectral domain immittance approach for dispersion characteristics of generalized printed transmission lines," *IEEE Trans. Microw. Theory Tech.*, vol. MTT-28, no. 7, pp. 733–736, Jul. 1980.
- [8] M. Abramowitz and I. A. Stegun, *Handbook of Mathematical Functions*. New York: Dover, 1965.
- [9] CST Microwave Studio V.5.0, Computer Simulation Technology, Germany.
- [10] R. Janaswamy, "An accurate moment method model for the tapered slot antenna," *IEEE Trans. Antennas Propagat.*, vol. 37, no. 12, pp. 1523–1528, Dec. 1989.
- [11] Advanced Design System, V.2008, Agilent Technology, USA.